

Enhancing Chain-of-Thought Reasoning with Critical Representation Fine-tuning

Chenxi Huang^{1,2*}, Shaotian Yan², Liang Xie^{2,3}, Binbin Lin^{4†},
Sinan Fan², Yue Xin², Deng Cai¹, Chen Shen^{2‡}, Jieping Ye²

¹the State Key Laboratory of CAD&CG, Zhejiang University

²Alibaba Cloud Computing

³College of Computer Science and Technology, Zhejiang University of Technology

⁴College of Software, Zhejiang University

Abstract

Representation Fine-tuning (ReFT), a recently proposed Parameter-Efficient Fine-Tuning (PEFT) method, has attracted widespread attention for significantly improving parameter efficiency by editing representation space alone. In this work, we investigate applying ReFT to complex reasoning tasks. However, directly using the native ReFT method, which modifies fixed representations at the beginning and end of each layer, yields suboptimal performance, as these fixed-position representations have uncertain impact on the outputs. We observe that, in complex reasoning tasks, there often exist certain critical representations. These representations either integrate significant information from preceding layers or regulate subsequent layer representations. Through layer-by-layer propagation, they exert a substantial influence on the final output. Naturally, fine-tuning these critical representations has the potential to greatly enhance reasoning performance. Building upon these insights, we propose **Critical Representation Fine-Tuning (CRFT)**, a novel method that identifies and optimizes these critical representations through information flow analysis. CRFT operates within a supervised learning framework, dynamically optimizing critical representations in a low-rank linear subspace while freezing the base model. The effectiveness and efficiency of our method are validated across eight benchmarks for arithmetic and commonsense reasoning, using LLaMA and Mistral model families. Notably, our method improves the accuracy of LLaMA-2-7B and ReFT by 18.2% and 3.8%, respectively, on GSM8K, while using only 0.016% of the model parameters, significantly less than other PEFT methods. Furthermore, our method also adapts effectively to few-shot settings, boosting one-shot accuracy by

*Work done during an internship at Alibaba Cloud Computing

†Correspondence: Binbin Lin<binbinlin@zju.edu.cn>, Chen Shen<jason.sc@alibaba-inc.com>

‡Project Lead.

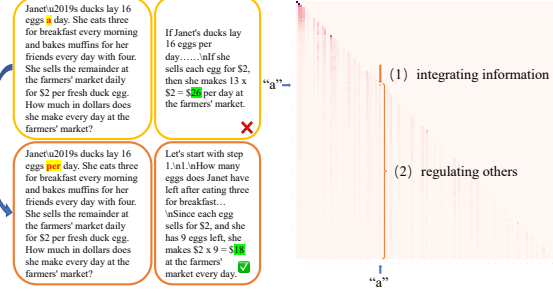


Figure 1: Examples of modifying a critical representation in the first layer (an input token). This example, conducted on LLaMA-2-13B, illustrates (1) two strategies of identifying critical representations and (2) the impact of modifying these representations on the output.

16.4%. Our work highlights the untapped potential of representation-level optimization for CoT reasoning, offering a lightweight yet powerful alternative to traditional PEFT methods.

1 Introduction

Large language models (LLMs) have made significant advances in the treatment of complex reasoning tasks (Chu et al., 2023; Yao et al., 2024; Besta et al., 2024), which demand intricate logical reasoning and comprehensive explanations. These tasks differ from simpler in-context tasks that mainly involve straightforward information retrieval or classification. A pivotal element in these advancements is the Chain-of-Thought (CoT) (Wei et al., 2022), decomposing the reasoning process into several intermediary steps, particularly used in the domains of arithmetic (Lu et al., 2022; Imani et al., 2023; Lightman et al., 2023) and commonsense (Trinh and Le, 2018; Ling et al., 2017; Patel et al., 2021).

Representation Fine-Tuning (ReFT) (Wu et al., 2024b) has emerged as a promising approach, offering parameter efficiency by operating at the representation level. Representations are considered fundamental as they reveal the inner reasoning processes of large language models (LLMs). However,

ReFT yields suboptimal performance in complex reasoning tasks, due to its reliance on altering fixed representations at the beginning and end of each layer, coupled with the unpredictable effects these changes have on the output. Through empirical analysis, we observe that in complex reasoning tasks, certain critical representations exist within each layer, as illustrated in Figure 1. These representations either aggregate significant information from the previous layer or modulate other representations in the subsequent layer. Through layer-by-layer propagation, they exert a substantial influence on the final reasoning output. To further validate their importance, introducing random perturbations (0.01 Gaussian noise) to a random representation in each layer of LLaMA-2-7B on GSM8K resulted in a 1.4% accuracy drop, underscoring the sensitivity of model performance to these representations. Naturally, fine-tuning these critical representations holds significant potential to enhance reasoning performance. Building upon these insights, we propose a novel PEFT method termed **Critical Representation Fine-Tuning (CRFT)**.

We employ information flow analytics (Wang et al., 2023), utilizing attention and saliency scores (Simonyan, 2013) as explicit indicators to identify critical representations. Specifically, for representations that aggregate significant information from the preceding layer, we prioritize those with predominant self-information flow, as they effectively consolidate gathered information. For representations that modulate subsequent layers, we focus on those with substantial outgoing information flow, reflecting their significant regulatory influence. However, optimizing critical representations poses a significant challenge due to their context-dependent nature. While some representations positively contribute to outputs and require no optimization, others adversely affect performance, with necessary adjustments varying across contexts. To address this, we introduce adaptive learning within a supervised framework. Building on recent advances in parameter-efficient fine-tuning (PEFT) at the representation level (Wu et al., 2024b,a), we freeze the base model and optimize critical representations by learning updated directions in a low-rank linear subspace.

We conducted comprehensive experiments on eight reasoning datasets in two scenarios: arithmetic and commonsense (Talmor et al., 2018), using four base models covering the LLaMA and Mistral families. The experimental results demonstrate

the effectiveness of our intervention. Specifically, our method achieves improvements of 18.2% over LLaMA-2-7B on the GSM8K dataset with only the 0.016% parameters of the model. Furthermore, our method can be easily extended to few-shot learning, achieving increases of 16.4% and 9.8% in one-shot and two-shot learning, respectively. Our work highlights the untapped potential of representation-level optimization for CoT reasoning, offering a lightweight yet powerful alternative to traditional prompt-centric and weight-centric methods.

2 Method

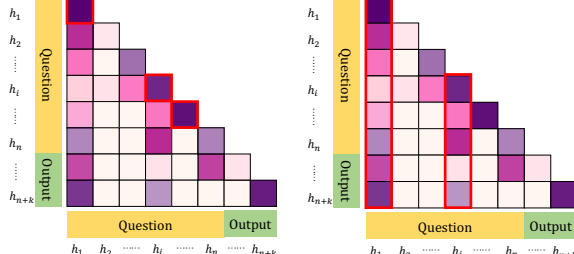
Our method, CRFT, consists of identifying and optimizing critical representations. We begin by introducing the problem formulation in Section 2.1. Next, we propose two strategies for identifying critical representations by analyzing the information flow, as presented in Section 2.2. Finally, we describe the way of optimizing critical representations in Section 2.3.

2.1 Problem Formulation

Given a sequence of n input tokens $\mathbf{x} = (x_1, \dots, x_n)$, the language model commences by embedding these tokens into a list of representations $\mathbf{h}^{(0)} = (\mathbf{h}_1^{(0)}, \dots, \mathbf{h}_n^{(0)})$. Since the vast majority of state-of-the-art language models are currently constructed based on the transformer (Vaswani, 2017) architecture, we focus solely on this architecture, which consists of L layers of transformer blocks. Subsequently, the L layers successively compute the l -th list of hidden representations $\mathbf{h}^{(l)}$ as a function of the previous list of hidden representations $\mathbf{h}^{(l-1)}$. Each hidden representation is a vector $\mathbf{h} \in \mathbb{R}^d$. Finally, the model leverages the last layer of hidden representations $\mathbf{h}^{(L)}$ to produce its predictions. Specifically, as a reasoning task, the model incrementally produces k tokens following the probability expression $p(x_{n+k}|x_1, \dots, x_n, x_{n+1}, \dots, x_{n+k-1})$. Our method aims to improve accuracy by identifying and optimizing critical representations $M(\mathbf{h})$.

2.2 Identify Critical Representations

Previous representation editing works also involve modification of representations but depend on empirical observations or general knowledge to locate representations for editing, which limits their adaptability and performance. For example, ReFT (Wu et al., 2024b) requires training and testing on other



(a) Self-referential filtering. (b) Multi-referential filtering.

Figure 2: The illustration of self-referential filtering and multi-referential filtering. We use red boxes to highlight the diagonal cells in Figure 2a and the column averages in Figure 2b that exceed the threshold α . The corresponding representations are marked with red lines and are referred to as critical representations.

datasets to determine the optimal number of continuous representations to edit, specified as the first x and last y representations. This selection process is not only cumbersome, but also lacks interpretability. Our work identifies critical representations $M(\mathbf{h})$, which significantly influence reasoning abilities and output correctness.

$$\begin{aligned} M(\mathbf{h}) = \{ & \mathbf{h}_i \mid \text{Is correct}(\text{model}(\mathbf{h}_i + \epsilon)) \\ & \neq \text{Is correct}(\text{model}(\mathbf{h}_i)) \}, \end{aligned} \quad (1)$$

where ϵ is a small perturbation in a vector space. For simplicity, we use the abbreviation $M^{(l)}$ to represent $M(\mathbf{h}^{(l)})$ in the following text. When all critical representations contribute positively to the output, accuracy is largely ensured.

As in the examples in Figure 1, whether a representation is a critical representation cannot be determined by itself but rather by its relationship with other representations. So, we utilize the information flow (Wang et al., 2023), leveraging attention and saliency scores as indicators. As shown in Figure 2, we use a grid to visualize the information interaction between representations, where cell (i, j) indicates the information interaction between representation j and representation i . The value of the cell (i, j) is indicated by attention scores or saliency scores, with darker colors signifying richer information interactions. The critical representations can be categorized into two functional roles: (1) integrating significant information from the preceding layer and (2) regulating the subsequent layer representations. Specifically, for the former, we focus on representations that consistently receive information flow from itself, indicating effective information accumulation. For the latter, we tar-

get representations that disseminate information to multiple others, indicating its rich information interaction. Consequently, we design two strategies to filter critical representations: *self-referential filtering* and *multi-referential filtering*, respectively.

2.2.1 Self-Referential Filtering

If information from representation i mainly flows back to itself in the subsequent layer, it means that representation i contains important information or has effectively accumulated significant information. Consequently, we use $\text{Info}(i, i)$ as a critical metric to assess this retention. If $\text{Info}(i, i)$ is large, then $\text{Info}(i, j), j \neq i$ will be small since the values in a row are normalized through the softmax function. This situation suggests that the information flow from the representation i is predominantly directed toward itself, confirming that the representation i is indeed crucial.

$$M_{\text{diag}}^{(l)} = \{ \mathbf{h}_i^{(l)} \mid \text{Info}^{(l-1)}(i, i) > \alpha, i \in \{1, \dots, n\} \}. \quad (2)$$

To quantify information interactions, we employ attention scores and saliency scores as indicators, thus proposing two distinct ways: Self-Referential Attention Filtering (SAF) and Self-Referential Saliency Filtering (SSF), separately.

Self-Referential Attention Filtering (SAF). We utilize normal attention scores $A_i^{(l)}$, described in Eq. 3, as an explicit indicator to filter critical representations, since they quantify the relevance and degree of emphasis assigned to various representations within a sequence. This mechanism enables the model to dynamically concentrate on interactions and enhance its understanding capabilities.

$$\text{Info}_{\text{SAF}}^{(l)}(i, i) = A_i^{(l)} = \text{softmax}(\mathbf{h}_i^{(l)} (\mathbf{h}^{(l)})^T / \sqrt{d}), \quad (3)$$

Self-Referential Saliency Filtering (SSF). We also leverage saliency scores to filter critical representations. As saliency score is a widely accepted interpretation tool (Simonyan, 2013), comprehensively considers attention scores and gradient values, highlighting interactions from critical representations to the model output, as shown in Eq. 4,

$$\text{Info}_{\text{SSF}}^{(l)}(i, i) = A_i^{(l)} \odot \frac{\partial \mathcal{L}(x)}{\partial A_i^{(l)}}, \quad (4)$$

where \odot denotes the element-wise multiplication, and $\mathcal{L}(\cdot)$ represents the cross entropy loss function of the predicted probability distribution and the predicted class indices.

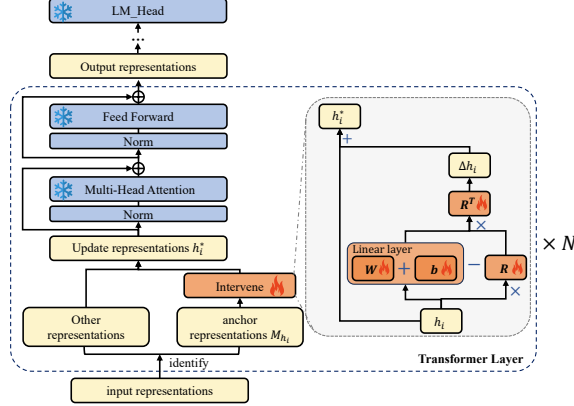


Figure 3: **The pipeline of optimizing critical representations.** Orange highlights the parameters to be learned, while blue indicates the parameters that remain frozen.

2.2.2 Multi-Referential Filtering

If information from representation j significantly affects multiple other representations, including producing representations, then representation j is crucial. Specifically, we calculate the average of cells in the column j as a critical metric to represent the influence of j on other representations. If the average of $\text{Info}(\cdot, j)$ is large, then representation j has a substantial influence on others and plays a crucial role. As shown in Eq. 5, we use the threshold β to filter the critical representations,

$$M_{\text{col}}^{(l)} = \left\{ h_j^{(l)} \mid \frac{\sum_{i=j}^{n+k} \text{Info}^{(l)}(i, j)}{n + k - j + 1} > \beta \right\}, \quad (5)$$

where k is the number of output representations.

We also use the attention score and the saliency score to quantify the influence of representation j on representation i , which is termed Multi-Referential Attention Filtering (MAF) and Multi-Referential Saliency Filtering (MSF), respectively.

2.3 Optimize Critical Representations

Upon identifying critical representations, it becomes imperative to optimize them to ensure that their influence on reasoning tasks is accurately aligned. However, the direction of this modification remains uncertain and may not be unique. Consequently, we model the adjustment as a learnable vector Δh , which is learned during the training process to rectify the critical representations adaptively. Following (Wu et al., 2024b; Huang et al., 2024), we restrict our optimized vectors to a low-rank linear subspace employing a projection matrix with orthonormal rows $R \in \mathbb{R}^{r \times d}$, where r indicates the dimensionality of the subspace we are intervening

PEFT	Param (%)	Identify	Accuracy (\uparrow)
None	-	-	14.6
LoRA (r=64)	0.826%	-	38.5
LoRA (r=8)	0.103%	-	36.7
RoSA ($r = 48$)	0.819%	-	30.5
RoSA ($r = 32$)	0.816%	-	32.2
RoSA ($r = 16$)	0.812%	-	32.8
SpA	0.809%	-	29.6
ReFT ($r = 8$)	0.031%	$p7 + s7$	29.0
		SAF	30.4 \uparrow 29.6
		MAF	32.0 \uparrow <u>32.1</u>
CRFT (ours)	0.016%	Union(attn)	31.2 \uparrow 32.8
		SSF	31.4 \uparrow 30.4
		MSF	31.4 \uparrow 30.3
		Union(sal)	32.8 \uparrow 31.5

Table 1: **Quantitative comparison of PEFT methods on GSM8K with LLaMA-2-7B.** The best performance is highlighted in **bold**, while the second-best is underlined.

in. We learn a projected source through a linear layer $\text{Linear}(h) = Wh + b$. Consequently, we modify the representation within the r -dimensional subspace spanned by the rows of R to adopt the values derived from our linear projection source, $\text{Linear}(h)$. The overall optimization mechanism is depicted in Eq. 6,

$$\Phi(h) = \begin{cases} h + R^T(Wh + b - Rh), & \text{if } h \in M(h) \\ h, & \text{otherwise.} \end{cases} \quad (6)$$

3 Experiments

To validate the effectiveness of our method, CRFT, we performed experiments in two scenarios covering eight datasets: GSM8K (Cobbe et al., 2021), AQuA (Ling et al., 2017), MAWPS (Koncel-Kedziorski et al., 2016), SVAMP (Patel et al., 2021), BoolQ (Clark et al., 2019), SocialIQA (Sap et al., 2019), WinoGrande (Sakaguchi et al., 2021), and OpenBookQA (Mihaylov et al., 2018). In particular, for the Commonsense task, previous work used the Commonsense170K dataset, which only provides the answers and lacks a reasoning process. We synthesized a Commonsense60K dataset with reasoning steps based on six commonly used commonsense datasets: CommonsenseQA (Talmor et al., 2018), CoS-e (Rajani et al., 2019), OpenBookQA (Mihaylov et al., 2018), SocialIQA (Sap et al., 2019), StrategyQA (Geva et al., 2021), WorldTree (Jansen et al., 2018). All experiments were conducted on the Pyvne (Wu et al., 2024c) codebase using a single GPU, either an NVIDIA

Model	PEFT	Identify	Accuracy (↑)						
			AQuA	MAWPS	SVAMP	BoolQ	SocialIQA	WinoGrande	OpenBookQA
LLaMA-2-7B	ReFT	p7+s7	21.7	80.7	52.2	50.7	61.2	51.7	58.6
		SAF	25.6 26.0	78.6 84.5	53.4 52.6	60.0 53.7	62.5 67.4	60.6 55.3	57.0 62.2
	CRFT (ours)	MAF	27.6 24.8	<u>81.1</u> 80.7	52.4 53.4	60.5 <u>61.8</u>	52.8 64.9	68.4 51.8	50.6 66.4
		SSF	26.0 26.8	80.7 79.8	52.5 <u>53.3</u>	62.0 54.3	67.1 64.4	60.2 60.1	58.4 58.6
		MSF	27.2 22.8	79.4 80.7	52.3 52.5	60.0 59.7	65.8 63.4	54.5 54.2	59.0 56.4
LLaMA-3-8B	ReFT	p7+s7	46.9	87.0	74.2	62.1	60.2	56.0	66.0
		SAF	47.2 47.2	89.9 88.2	75.5 76.1	63.0 66.4	68.2 67.1	62.6 56.3	71.0 73.6
	CRFT (ours)	MAF	48.4 <u>50.4</u>	90.8 90.8	77.1 77.9	62.4 66.2	66.5 62.7	67.2 <u>62.9</u>	73.8 72.6
		SSF	50.0 49.2	86.6 86.6	78.0 78.1	64.0 66.6	74.7 74.2	60.3 62.0	75.6 77.0
		MSF	48.0 51.6	87.0 87.4	75.2 74.8	<u>67.0</u> 67.9	67.4 69.7	62.3 62.8	70.0 68.6
Mistral-7B	ReFT	p7+s7	32.3	84.9	67.4	62.5	64.6	58.5	63.8
		SAF	36.2 38.6	87.0 85.7	65.9 66.2	63.0 66.5	66.7 75.6	61.5 62.9	72.6 72.6
	CRFT (ours)	MAF	<u>39.0</u> 38.2	84.9 85.3	66.3 65.3	62.1 60.8	66.9 71.5	61.2 <u>63.7</u>	64.2 69.6
		SSF	37.4 33.5	85.3 84.5	<u>70.3</u> 70.6	62.3 64.8	64.9 62.9	64.3 61.4	61.6 66.4
		MSF	41.3 37.8	87.4 85.3	66.0 66.9	62.5 <u>65.0</u>	69.3 <u>71.8</u>	62.3 59.5	72.8 68.6

Table 2: **Quantitative comparison on arithmetic and commonsense reasoning datasets with three base models: LLaMA-2-7B, LLaMA-3-8B, and Mistral-7B.** We train on Math10k and report results on AQuA, MAWPS, and SVAMP for arithmetic reasoning datasets; and we train on our combined commonsense datasets Commonsense60k and report results on four datasets: BoolQ, SocialIQA, WinoGrande, and OpenBookQA.

A100 (80GB) or an L20 (40GB). And our method requires 4 hours for training on GSM8K with LLaMA-2-7B. We set the scoring method to the “order”, with α and β both set to 0.05. The ablation studies of these hyperparameters are discussed in Section 3.3. We adopt SAF strategy in Section 3.2 and Section 3.3. The details of all datasets and other implementations are reported in Appendix A. Our evaluation focused exclusively on the accuracy of the final numerical or multiple-choice answers. Generation examples are reported in Appendix C.

3.1 Quantitative Results

Table 1 summarizes the comparison of our method, CRFT, with other PEFT methods on GSM8k with LLaMA-2-7B. For each strategy, we report two accuracy values: the first value involves selecting critical representations by further filtering those identified as critical representations from the previous layer, while the second value focuses on identifying critical representations by filtering only within the current layer. Given that the optimal strategy may differ by context, we recommend a combined approach of self-referential and multi-referential filtering. Since the scoring systems of these two strategies are not directly comparable, the union of the filtered sets is employed. To ensure a fair comparison, the same number of critical representations is maintained, which may lead to the omission of some highly important ones. Consequently,

the combined method may exhibit slightly lower performance in certain situations. Alternatively, adjusting the threshold α and β provides a solution: lowering α (β) increases interventions for improved performance, while raising α (β) decreases interventions for enhanced efficiency.

Without bells and whistles, our method is comparable with other PEFT methods with fewer learnable parameters. For example, one of our strategies, union with attention scores, outperforms LLaMA-2-7B and ReFT by 18.2% and 3.8%, respectively. Furthermore, the percentage of trainable parameters, calculated by dividing the trainable parameters by the total parameters of the model, highlights their substantial efficiency. Our method requires only 1/6 of the learnable parameters used by LoRA and 1/2 of those used by ReFT with the same rank.

Furthermore, our method, CRFT, consistently exhibits better performance on different models in arithmetic and commonsense scenarios. We report the results on different model sizes and model families on GSM8K: LLaMA-2-7B, LLaMA-2-13B, LLaMA-3-8B, and Mistral-7B, as shown in Appendix B.1. In addition, we present additional experimental results in arithmetic and commonsense scenarios, as shown in Table 2. We use the official public code of ReFT to report performance, as it only reports the results on LLaMA-1. And following the experimental conclusion of ReFT, we adopt the best intervention

Few-shot	zero-shot	one-shot	two-shot
None	14.6	16.2	20.5
CRFT	29.6	28.7 32.6	29.0 30.3
Improvement	+15.0	+12.5 +16.4	+8.5 +9.8

Table 3: Expand our method to few-shot learning on GSM8K using Llama-2-7B with the SAF strategy.

Threshold	1.0	0.25	0.05	0.01
Accuracy (\uparrow)	24.7	30.0	29.6	33.2

Table 4: Ablation study on threshold α (β) on GSM8K using Llama-2-7B with the SAF strategy.

parameters $p7 + s7$, indicating the intervention in the first and the last seven representations. The consistent improvements observed in different reasoning tasks and different models underscore the robustness and versatility of our approach.

3.2 Expand to Few-shot Learning

Our method can easily be extended to few-shot learning. Intuitively, demonstrations should not directly affect the output; they are usually used to gain a higher-level semantic understanding, which then affects the output. However, representations in the question, such as numbers, can indeed have a direct impact. Consequently, we present experiments in Table 3 to examine whether the demonstration and the question should be learned independently. The first value suggests that the demonstration and the question are interdependent, leading to a single update vector for the critical representations. Conversely, the second value implies that the demonstration and the question are independent, resulting in distinct update vectors. These results prove the necessity of differentiating update directions between demonstrations and the question. Due to memory limitation, we only experimented with one-shot and two-shot.

3.3 Hyperparameter Configurations

We conducted extensive ablation studies on GSM8K using Llama-2-7B with the SAF strategy to systematically investigate hyperparameters, including the threshold α and β , the number of intervention representations and selection criteria.

The threshold α and β determines the degree to which the critical representations are. Given that the threshold values for α and β lie on the same dimension, we apply a unified threshold for both self-referential filtering and multi-referential

Number	0	14	20	30
Accuracy (\uparrow)	14.6	29.6	30.3	27.7

Table 5: Ablation study on the number of intervention representations on GSM8K using Llama-2-7B with the SAF strategy.

Criteria	order	score	random
Accuracy (\uparrow)	29.6	28.7	23.1

Table 6: Ablation study on selection criteria on GSM8K using Llama-2-7B with the SAF strategy.

filtering. We investigated four values, as shown in Table 4, and found that a threshold of 0.01 yields the best results. As the threshold decreases, the number of selected representations increases, but altering these selected representations can be more difficult. However, a lower threshold also carries the risk of excluding significant representations.

In the implementation, the number of intervention representations for each layer is fixed. If the number of critical representations obtained through the SAF strategy exceeds the number of intervention representations, we sample them using specific selection criteria. Conversely, if the number of critical representations is fewer than needed, we use a placeholder value of -1 to pad the length. For a fair comparison with the ReFT method, we set the default number of intervention representations to 14. An ablation study on the number of representations, shown in Table 5, revealed that the results were optimal when set to 20. When the number of intervention representations becomes too large, it hinders the learning of the update direction, leading to suboptimal results compared to using fewer representations.

For selection criteria, we designed three approaches to sample critical representations: positional order, score ranking, and random selection. The results, shown in Table 6, indicate that positional order selection is superior, while random selection yields significantly lower results compared to the other two criteria.

The ablation study presented above suggests that careful selection of hyperparameters can further enhance the performance of our CRFT method.

3.4 Are critical representations instrumental?

We validate that the selected representations are critical representations with a significant impact on the output. Using SAF as an identification strategy,

Layer	None	0	31	0-15	16-31	all
Acc. (\uparrow)	14.6	24.9	22.7	30.5	24.6	29.6

Table 7: **The validation of effectiveness in each layer on GSM8K using Llama-2-7B with the SAF strategy.**

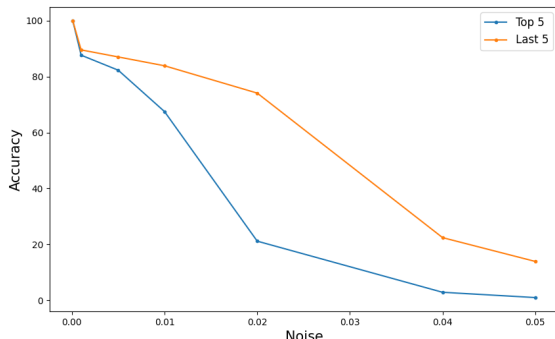


Figure 4: **The validation of critical representations identification.** Accuracy of originally correct examples under noise in the top 5 and last 5 representations.

we selected the top 5 and last 5 representations based on their scores for each layer on GSM8K with LLaMA-2-7B. The effects of adding noise to these representations are presented in Figure 4, where the x-axis represents the magnitude of the noise, and the y-axis shows the proportion of originally correct examples remaining correct. We observe that the accuracy of the top 5 representations decreases rapidly with increasing noise. When the noise level is 0.02, the accuracy of the top 5 representations drops to 21.1%, whereas the last 5 representations maintain an accuracy of 74.1%. This result demonstrates the significant impact of critical representations on output performance.

In addition, we investigated the necessity of identifying critical representations. We tested random intervention locations using seed values ranging from 37 to 47. As shown in Table 8, the interventions of random representations during training can surpass the original LLaMA-2-7B, as the update direction is learnable. However, it remains inferior to the results achieved through our careful identification of critical representations, highlighting the necessity of this process.

Furthermore, we verified that intervention is necessary at each layer. As shown in Table 7, we intervene in the first layer (Layer 0), the final layer (Layer 31), the first half of the layers [0 – 15], the last half of the layers [16 – 31], and all layers. We found that each intervention improved accuracy and that interventions in the earlier layers have a greater impact on the results. However, the best per-

formance was achieved by intervening in the first half of the layers, as earlier feature representations are more closely aligned with the task objectives and can propagate throughout the model.

3.5 How do critical representations impact information flow?

We visualize attention maps to capture the variations in the information flow. The first and last heads in the final layer (Layer 32) of both LLaMA-2-7B and our proposed method, CRFT (SAF), are illustrated in Figure 5. A comprehensive comparison of all heads is provided in Appendix D, and the phenomenon is consistent. We have identified three observations, as follows:

- **Excessive information interaction in the representation h_0 is reduced.** In column 0, the absence of prominent color indicates a diminished influence of representation h_0 on other representations. The initial representation h_0 in LLaMA-2-7B lacks semantic information, but attracts a high level of attention. Previous works (Xiao et al., 2023; Yu et al., 2024) have referred to this phenomenon as the “attention sink”. By applying our method, the representation h_0 receives less undue attention, leading to a more balanced distribution of attention.
- **Increased information interaction between representations.** The increase in the number of vertical lines signifies a heightened interaction among the representations.
- **Broader information flow.** The presence of high attention scores along the diagonal has shifted from a few isolated peaks to multiple cells. This denotes a broader information flow from various representations.

Based on the visualized results above, our method alters the direction of information flow, guiding it towards a more optimal path, and enriching the overall information interaction.

4 Related Work

Intervention in LLMs. Intervention strategies encompass various techniques designed to influence the behavior of large-scale models during the inference phase. Common strategies include activation editing (Li et al., 2024), weight editing (Dai et al., 2022), and the use of guidance vectors (Zou et al.,

Location	None	ReFT	Our CRFT	Uniform Random										
	$(p7 + s7)$	(MAF)	37	38	39	40	41	42	43	44	45	46	47	
Accuracy (\uparrow)	14.6	29.0	32.1	26.6	26.6	28.1	27.3	25.5	24.5	27.8	27.5	28.1	26.2	26.4

Table 8: **The necessity of identifying critical representations.** We present the results with LLaMA-2-7B on GSM8K. The best way to identify critical representations is highlighted in **bold**, while the second-best is underlined.

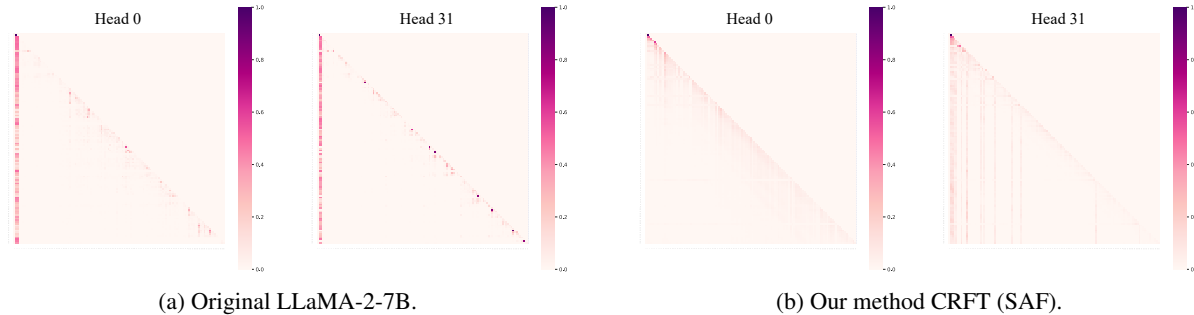


Figure 5: **Visualization of attention scores for the first and last heads in the last layer.**

2023), as well as altering the output distribution through comparative analysis (Li et al., 2022; Chuang et al., 2023). As representations encode rich information, some methods (Geiger et al., 2021; Wu et al., 2024b; AlKhamissi et al., 2024) change the output by editing representations. Although representation interventions can serve as powerful tools for model control, previous methods intervene in representations based on empirical observations (Wu et al., 2024a,b) or general knowledge (Zhang et al., 2023). The above approaches are not general and time-consuming, which limits their adaptability and performance. In contrast, our method precisely identifies the representations to intervene.

Information Flow Analysis. Recent studies (Yuan et al.; Yan et al.; Fan et al.) have utilized attention mechanisms to analyze their impact on model performance. For example, StreamLLM (Xiao et al., 2023) discovered that the initial token of an input text often receives an excessive amount of attention, despite frequently lacking semantic significance. It suggests that we should preserve these tokens when processing long input sequences to prevent forgetting. Furthermore, ACT (Yu et al., 2024) found that attention sinks can occur not only at the initial token but also throughout the entire sequence. Moreover, it was discovered that these attention sinks are not always beneficial to model performance. ACT optimizes attention distributions during inference, but not all heads can benefit from the calibration. Similarly, PASTA (Zhang et al., 2023) demonstrates that increasing the attention score of

defined tokens in specific heads can improve the ability of LLM to follow instructions. However, tokens need to be manually defined. Our method addresses these challenges by adaptively learning the updated direction of critical representations during training, leading to better overall performance.

5 Conclusion

We propose a novel Chain-of-Thought (CoT) reasoning method, termed Critical Representation Fine-Tuning (CRFT), which focuses exclusively on critical representations to influence model outputs. CRFT first identifies critical representations by analyzing the information flow through attention and saliency scores, and subsequently optimizes them via supervised fine-tuning within a low-rank subspace. Comprehensive experiments conducted across various models and datasets validate the effectiveness and efficiency, providing a new perspective on CoT reasoning tasks, particularly in long CoTs. Furthermore, CRFT exhibits sufficient flexibility to be readily adapted to a few-shot learning scenarios, underscoring its potential to enhance reasoning capabilities within models.

Limitation

For identification, we currently focus on searching for representations that significantly impact the model output. However, it is important to note that representations with minor impacts may still have an influence, even if their effects are often negligible. A more effective strategy could involve

prioritizing the correction of representations with negative impacts, although identifying such representations remains a challenge. Furthermore, while our optimizations are currently restricted to linear spaces, there is potential to explore alternative optimization methods that could enhance our framework.

Acknowledgements

This work was supported in part by the National Nature Science Foundation of China (Grant Nos: 62273302, 62273303, 62036009), in part by the Yongjiang Talent Introduction Programme (Grant Nos.: 2022A-240-G), in part by Ningbo Key R&D Program (Nos.: 2023Z231, 2023Z229), in part by the Alibaba Research Intern Program. We sincerely thank Lei Li for his suggestions in writing.

References

- Badr AlKhamissi, Greta Tuckute, Antoine Bosselut, and Martin Schrimpf. 2024. The llm language network: A neuroscientific approach for identifying causally task-relevant units. *arXiv preprint arXiv:2411.02280*.
- Maciej Besta, Nils Blach, Ales Kubicek, Robert Gerstenberger, Michal Podstawski, Lukas Gianinazzi, Joanna Gajda, Tomasz Lehmann, Hubert Niewiadomski, Piotr Nyczyk, and 1 others. 2024. Graph of thoughts: Solving elaborate problems with large language models. In *Proceedings of the AAAI Conference on Artificial Intelligence*, volume 38, pages 17682–17690.
- Zheng Chu, Jingchang Chen, Qianglong Chen, Weijiang Yu, Tao He, Haotian Wang, Weihua Peng, Ming Liu, Bing Qin, and Ting Liu. 2023. A survey of chain of thought reasoning: Advances, frontiers and future. *arXiv preprint arXiv:2309.15402*.
- Yung-Sung Chuang, Yujia Xie, Hongyin Luo, Yoon Kim, James Glass, and Pengcheng He. 2023. Dola: Decoding by contrasting layers improves factuality in large language models. *arXiv preprint arXiv:2309.03883*.
- Christopher Clark, Kenton Lee, Ming-Wei Chang, Tom Kwiatkowski, Michael Collins, and Kristina Toutanova. 2019. Boolq: Exploring the surprising difficulty of natural yes/no questions. *arXiv preprint arXiv:1905.10044*.
- Karl Cobbe, Vineet Kosaraju, Mohammad Bavarian, Mark Chen, Heewoo Jun, Lukasz Kaiser, Matthias Plappert, Jerry Tworek, Jacob Hilton, Reiichiro Nakano, Christopher Hesse, and John Schulman. 2021. Training verifiers to solve math word problems. *arXiv preprint arXiv:2110.14168*.
- Damai Dai, Yutao Sun, Li Dong, Yaru Hao, Shuming Ma, Zhifang Sui, and Furu Wei. 2022. Why can gpt learn in-context? language models implicitly perform gradient descent as meta-optimizers. *arXiv preprint arXiv:2212.10559*.
- Sinan Fan, Liang Xie, Chen Shen, Ge Teng, Xiaosong Yuan, Xiaofeng Zhang, Chenxi Huang, Wenxiao Wang, Xiaofei He, and Jieping Ye. Improving complex reasoning with dynamic prompt corruption: A soft prompt optimization approach. In *The Thirteenth International Conference on Learning Representations*.
- Atticus Geiger, Hanson Lu, Thomas Icard, and Christopher Potts. 2021. Causal abstractions of neural networks. *Advances in Neural Information Processing Systems*, 34:9574–9586.
- Mor Geva, Daniel Khashabi, Elad Segal, Tushar Khot, Dan Roth, and Jonathan Berant. 2021. Did Aristotle Use a Laptop? A Question Answering Benchmark with Implicit Reasoning Strategies. *Transactions of the Association for Computational Linguistics (TACL)*.
- Zhiqiang Hu, Lei Wang, Yihuai Lan, Wanyu Xu, Ee-Peng Lim, Lidong Bing, Xing Xu, Soujanya Poria, and Roy Ka-Wei Lee. 2023. Llm-adapters: An adapter family for parameter-efficient fine-tuning of large language models. *arXiv preprint arXiv:2304.01933*.
- Jing Huang, Zhengxuan Wu, Christopher Potts, Mor Geva, and Atticus Geiger. 2024. Ravel: Evaluating interpretability methods on disentangling language model representations. *arXiv preprint arXiv:2402.17700*.
- Shima Imani, Liang Du, and Harsh Shrivastava. 2023. Mathprompter: Mathematical reasoning using large language models. *arXiv preprint arXiv:2303.05398*.
- Peter A Jansen, Elizabeth Wainwright, Steven Marmorstein, and Clayton T Morrison. 2018. Worldtree: A corpus of explanation graphs for elementary science questions supporting multi-hop inference. *arXiv preprint arXiv:1802.03052*.
- Rik Koncel-Kedziorski, Subhro Roy, Aida Amini, Nate Kushman, and Hannaneh Hajishirzi. 2016. **MAWPS: A math word problem repository**. In *Proceedings of the 2016 Conference of the North American Chapter of the Association for Computational Linguistics: Human Language Technologies*, pages 1152–1157, San Diego, California. Association for Computational Linguistics.
- Jiachun Li, Pengfei Cao, Chenhao Wang, Zhuoran Jin, Yubo Chen, Daojian Zeng, Kang Liu, and Jun Zhao. 2024. Focus on your question! interpreting and mitigating toxic cot problems in commonsense reasoning. *arXiv preprint arXiv:2402.18344*.
- Xiang Lisa Li, Ari Holtzman, Daniel Fried, Percy Liang, Jason Eisner, Tatsunori Hashimoto, Luke Zettlemoyer, and Mike Lewis. 2022. Contrastive decoding: Open-ended text generation as optimization. *arXiv preprint arXiv:2210.15097*.
- Hunter Lightman, Vineet Kosaraju, Yura Burda, Harry Edwards, Bowen Baker, Teddy Lee, Jan Leike, John Schulman, Ilya Sutskever, and Karl Cobbe. 2023. Let’s verify step by step. *arXiv preprint arXiv:2305.20050*.
- Wang Ling, Dani Yogatama, Chris Dyer, and Phil Blunsom. 2017. Program induction by rationale generation: Learning to solve and explain algebraic word problems. *arXiv preprint arXiv:1705.04146*.
- Pan Lu, Liang Qiu, Kai-Wei Chang, Ying Nian Wu, Song-Chun Zhu, Tanmay Rajpurohit, Peter Clark, and Ashwin Kalyan. 2022. Dynamic prompt learning via policy gradient for semi-structured mathematical reasoning. *arXiv preprint arXiv:2209.14610*.
- Todor Mihaylov, Peter Clark, Tushar Khot, and Ashish Sabharwal. 2018. Can a suit of armor conduct electricity? a new dataset for open book question answering. *arXiv preprint arXiv:1809.02789*.

- Arkil Patel, Satwik Bhattacharya, and Navin Goyal. 2021. Are nlp models really able to solve simple math word problems? *arXiv preprint arXiv:2103.07191*.
- Nazneen Fatema Rajani, Bryan McCann, Caiming Xiong, and Richard Socher. 2019. Explain yourself! leveraging language models for commonsense reasoning. In *Proceedings of the 2019 Conference of the Association for Computational Linguistics (ACL2019)*.
- Keisuke Sakaguchi, Ronan Le Bras, Chandra Bhagavatula, and Yejin Choi. 2021. Winogrande: An adversarial winograd schema challenge at scale. *Communications of the ACM*, 64(9):99–106.
- Maarten Sap, Hannah Rashkin, Derek Chen, Ronan LeBras, and Yejin Choi. 2019. Socialqa: Commonsense reasoning about social interactions. *arXiv preprint arXiv:1904.09728*.
- Karen Simonyan. 2013. Deep inside convolutional networks: Visualising image classification models and saliency maps. *arXiv preprint arXiv:1312.6034*.
- Alon Talmor, Jonathan Herzig, Nicholas Lourie, and Jonathan Berant. 2018. Commonsenseqa: A question answering challenge targeting commonsense knowledge. *arXiv preprint arXiv:1811.00937*.
- Trieu H Trinh and Quoc V Le. 2018. A simple method for commonsense reasoning. *arXiv preprint arXiv:1806.02847*.
- A Vaswani. 2017. Attention is all you need. *Advances in Neural Information Processing Systems*.
- Lean Wang, Lei Li, Damai Dai, Deli Chen, Hao Zhou, Fandong Meng, Jie Zhou, and Xu Sun. 2023. Label words are anchors: An information flow perspective for understanding in-context learning. *arXiv preprint arXiv:2305.14160*.
- Jason Wei, Xuezhi Wang, Dale Schuurmans, Maarten Bosma, Fei Xia, Ed Chi, Quoc V Le, Denny Zhou, and 1 others. 2022. Chain-of-thought prompting elicits reasoning in large language models. *Advances in neural information processing systems*, 35:24824–24837.
- Muling Wu, Wenhao Liu, Xiaohua Wang, Tianlong Li, Changze Lv, Zixuan Ling, Jianhao Zhu, Cenyuan Zhang, Xiaoqing Zheng, and Xuanjing Huang. 2024a. Advancing parameter efficiency in fine-tuning via representation editing. *arXiv preprint arXiv:2402.15179*.
- Zhengxuan Wu, Aryaman Arora, Zheng Wang, Atticus Geiger, Dan Jurafsky, Christopher D Manning, and Christopher Potts. 2024b. Reft: Representation finetuning for language models. *arXiv preprint arXiv:2404.03592*.
- Zhengxuan Wu, Atticus Geiger, Aryaman Arora, Jing Huang, Zheng Wang, Noah Goodman, Christopher Manning, and Christopher Potts. 2024c. `pyvne`: A library for understanding and improving PyTorch models via interventions. In *Proceedings of the 2024 Conference of the North American Chapter of the Association for Computational Linguistics: Human Language Technologies (Volume 3: System Demonstrations)*, pages 158–165, Mexico City, Mexico. Association for Computational Linguistics.
- Guangxuan Xiao, Yuandong Tian, Beidi Chen, Song Han, and Mike Lewis. 2023. Efficient streaming language models with attention sinks. *arXiv preprint arXiv:2309.17453*.
- Shaotian Yan, Chen Shen, Wenxiao Wang, Liang Xie, Junjie Liu, and Jieping Ye. Don’t take things out of context: Attention intervention for enhancing chain-of-thought reasoning in large language models. In *The Thirteenth International Conference on Learning Representations*.
- Shunyu Yao, Dian Yu, Jeffrey Zhao, Izhak Shafran, Tom Griffiths, Yuan Cao, and Karthik Narasimhan. 2024. Tree of thoughts: Deliberate problem solving with large language models. *Advances in Neural Information Processing Systems*, 36.
- Zhongzhi Yu, Zheng Wang, Yonggan Fu, Huihong Shi, Khalid Shaikh, and Yingyan Celine Lin. 2024. Unveiling and harnessing hidden attention sinks: Enhancing large language models without training through attention calibration. *arXiv preprint arXiv:2406.15765*.
- Xiaosong Yuan, Chen Shen, Shaotian Yan, Xiao Feng Zhang, Liang Xie, Wenxiao Wang, Renchu Guan, Ying Wang, and Jieping Ye. Instance-adaptive zero-shot chain-of-thought prompting. In *The Thirty-eighth Annual Conference on Neural Information Processing Systems*.
- Qingru Zhang, Chandan Singh, Liyuan Liu, Xiaodong Liu, Bin Yu, Jianfeng Gao, and Tuo Zhao. 2023. Tell your model where to attend: Post-hoc attention steering for llms. *arXiv preprint arXiv:2311.02262*.
- Andy Zou, Long Phan, Sarah Chen, James Campbell, Phillip Guo, Richard Ren, Alexander Pan, Xuwang Yin, Mantas Mazeika, Ann-Kathrin Dombrowski, and 1 others. 2023. Representation engineering: A top-down approach to ai transparency. *arXiv preprint arXiv:2310.01405*.

A Implement Details

A.1 Datasets

The test datasets that we use across two scenarios covering eight datasets: GSM8K (Cobbe et al., 2021), AQuA (Ling et al., 2017), MAWPS (Koncel-Kedziorski et al., 2016), SVAMP (Patel et al., 2021), BoolQ (Clark et al., 2019), SocialIQA (Sap et al., 2019), WinoGrande (Sakaguchi et al., 2021), and OpenBookQA (Mihaylov et al., 2018).

GSM8K. GSM8K, which comprises grade-school math word problems requiring multi-step reasoning, usually takes between 2 and 8 steps to solve problems using basic arithmetic operations $+, -, \times, \div$. We used the last 300 samples in the training set as the validation set and reported the results on its test set.

Arithmetic Reasoning Scenarios. Following the experimental setup established in Hu et al. (2023), we fine-tune a combined dataset of seven arithmetic reasoning tasks, called Math10K, utilizing LM-generated chain-of-thought steps. We report performance metrics in three test sets: AQuA, MAWPS, and SVAMP.

Commonsense Reasoning Scenarios. For commonsense reasoning scenarios, we opted not to use Commonsense170K from Hu et al. (2023), as it does not incorporate CoT steps. We create a suitable Commonsense60k training set, combining six commonsense reasoning tasks: CommonsenseQA (Talmor et al., 2018), CoS-e (Rajani et al., 2019), OpenBookQA (Mihaylov et al., 2018), SocialIQA (Sap et al., 2019), StrategyQA (Geva et al., 2021), WorldTree (Jansen et al., 2018). We report performance metrics in four test sets: BoolQ, SocialIQA, WinoGrande, and OpenBookQA.

A.2 Base Models

We finetune our models on LLaMA-2-7B, LLaMA-2-13B, LLaMA-3-8B and Mistral-7B. We use the “chat” version of LLaMA-2, and the “instruct” version of LLaMA-3 and Mistral-7B.

A.3 Hyperparameters

For a fair comparison with ReFT ($p7 + s7$), we selected 14 intervention representations and maintained a rank of 8, consistent with the parameters used in ReFT. We set the hyperparameters of α to 0.05. And we used the “order” selection criteria by default. To ensure a fair comparison, we maintain the same training principle, details are shown in

HyperParameters	Values
Rank	8
Number of representations	14
threshold α	0.05
selection criteria	Order(default)
Number of Epochs	12 for arithmetic, 6 for commonsense
Batch Size	2
Gradient accumulation steps	16
seed	42
Optimizer	AdamW
Learning Rate Schedule	Linear
Learning Rate	$9e - 4$
dropout	0.05 for GSM8K, 0 for others
Weight Decay	0.06 for GSM8K, 0 for others
Warmup ratio	0 for GSM8K, 0.1 for others

Table 9: The values of hyperparameters.

Table 9. For all tasks, model outputs are generated with greedy search.

A.4 Prompt

We use a prompt for each task.

GSM8K
[question] Answer the above question. First, think step by step and then answer the final number.
Other Arithmetic Scenario
Below are instructions for a task. Write a response that appropriately completes the request. ### Instruction: [Question] ### Response:
Commonsense Scenario
[Question] the correct answer is

B Further Ablation Studies

To further demonstrate the effectiveness of our proposed method CRFT, we provide additional experimental results.

B.1 Performance under Different Base Models

We verify our method, CRFT, in different models, as shown in Table 10. We tested four basic models (LLaMA-2-7B, LLaMA-2-13B, LLaMA-3-8B,

PEFT	Identify	Accuracy (\uparrow)			
		LLaMA-2-7B	LLaMA-2-13B	LLaMA-3-8B	Mistral-7B
None	-	14.6	30.9	64.5	38.4
ReFT	p7+s7	29.0	37.9	64.7	46.5
	SAF	30.4 29.6	38.7 39.6	<u>70.8</u> 70.6	46.4 46.9
	MAF	32.0 <u>32.1</u>	38.3 38.0	67.5 64.8	48.0 47.3
	Union(attn)	31.2 32.8	40.3 39.4	64.4 71.0	<u>48.1</u> 47.7
	SSF	31.4 30.4	<u>40.1</u> 38.4	64.6 64.5	46.4 46.5
	MSF	31.4 30.3	38.3 38.3	64.5 65.1	46.9 47.7
	Union(sal)	32.8 31.5	38.3 38.3	63.8 64.0	48.0 48.2

Table 10: **Quantitative comparison on GSM8K with four base models: LLaMA-2-7B, LLaMA-2-13B, LLaMA-3-8B, and Mistral-7B.** The best performance is highlighted in **bold**, while the second-best is underlined.

Mistral-7B) on the GSM8K dataset, covering different sizes and families. The consistent improvement of our experimental results demonstrates the effectiveness of our method.

PEFT	Identify	Accuracy (\uparrow)
ReFT	-	29.0
	SAF	31.1 33.1
	MAF	32.2 30.3
	Union(attn)	<u>32.9</u> 32.9
	SSF	32.0 32.2
	MSF	31.8 30.0
	Union(attn)	30.6 31.8

Table 11: **Quantitative performance on GSM8K using LLaMA-2-7B with $\alpha = 0.01$.**

B.2 Performance under Optimized Parameter Configuration

We present the performance of our approach on the GSM8K dataset using the LLaMA-2-7B base model with an optimized threshold of 0.01 in Table 11. These results indicate that setting the threshold to 0.01 indeed leads to improved performance.

B.3 Efficacy of the Union Strategy

We present supplementary experiments to validate the efficacy of the Union strategy, in Table 12. Specifically, we evaluate our method on the AQuA (mathematics) and BoolQ (commonsense reasoning) datasets, employing both LLaMA-2-7B and LLaMA-3-8B as base models. The results demonstrate that the Union strategy consistently achieves gains without requiring manual selection.

C Generation Examples

We give a generation example for each test dataset.

D Attention Analysis

We visualize the attention score of all 32 heads in the final layer and the last head in all layers, which illustrates that our method indeed enriches information interactions.

PEFT	Identify	Accuracy (\uparrow)			
		AQuA		BoolQ	
		LLaMA-2-7B	LLaMA-3-8B	LLaMA-2-7B	LLaMA-3-8B
ReFT	-	21.7	46.9	50.7	62.1
CRFT(ours)	SAF	25.6 26.0	47.2 47.2	60.0 53.7	63.0 64.4
	MAF	27.6 24.8	48.4 50.4	60.5 61.8	62.4 66.2
	Union(attn)	<u>28.4</u> 30.3	49.6 <u>53.2</u>	57.4 57.5	69.4 66.4
	SSF	26.0 26.8	50.0 49.2	62.0 54.3	64.0 66.6
	MSF	27.2 22.8	48.0 51.6	60.0 59.7	67.0 67.9
	Union(sal)	26.8 27.6	53.5 <u>53.2</u>	59.7 61.7	<u>68.8</u> 67.8

Table 12: **The efficacy of the union strategy.** We present the results with LLaMA-2-7B and LLaMA-3-8B on AQuA and BoolQ. The best performance is highlighted in **bold**, while the second-best is underlined.

Instruction (GSM8K)

Marie ordered one chicken meal that costs \$12, 5 packs of milk that costs \$3 each, 4 apples that cost \$1.50 each, and some boxes of pizza. Marie paid a total of \$50. How many boxes of pizza did Marie order if each box costs \$8.50?

Response	
Model Response	
LLaMA-2-7B	Great, let's break it down step by step to find out how many boxes of pizza Marie ordered: 1. First, let's calculate the total cost of Marie's meal: $\$12 \text{ (chicken meal)} + \$15 \text{ (5 packs of milk)} = \27 2. Next, let's calculate the total cost of Marie's fruits: $\$1.50 \text{ (4 apples)} = \6 3. Now, let's add the total cost of Marie's meal and fruits: $\$27 + \$6 = \$33$ 4. Finally, let's subtract the total cost of Marie's meal and fruits from the total amount she paid: $\$50 - \$33 = \$17$ So, Marie ordered \$17 worth of pizza boxes, which is equal to 4 boxes (since each box costs \$8.50). Therefore, the answer is 4 boxes of pizza.
ReFT	Marie paid a total of $\$12 + \$3 \times 5 = \$25$ for the milk. She paid a total of $\$15 + \$1.50 \times 4 = \$19$ for the apples. So, Marie paid a total of $\$50 - \$25 - \$19 = \16 for the pizza. Therefore, Marie ordered $\$16 / \$8.50 = 2$ boxes of pizza. The final answer is: 2
CRFT	The cost of 5 packs of milk is $\$3 \times 5 = \15 . The cost of 4 apples is $\$1.50 \times 4 = \6 . The total cost of the chicken meal, milk, and apples is $\$12 + \$15 + \$6 = \33 . So, Marie ordered $\$50 - \$33 = \$17$ worth of pizza. Therefore, Marie ordered $\$17 / \$8.50 = 2$ boxes of pizza. The final answer is: 2

Instruction (AQuA)

Two ants are standing side-by-side. One ant, which is 4 inches tall, casts a shadow that is 10 inches long. The other ant is 6 inches tall. Compute, in inches, the length of the shadow that the taller ant casts. Answer Choices: (A) 36 (B) 28 (C) 42 (D) 15 (E) 20

Response

Model	Response
LLaMA-2-7B	<p>Great, I'd be happy to help you with that!</p> <p>According to the instruction, the length of the ribbon was originally 30 cm and it was reduced in the ratio 5 : 3. To find the length of the ribbon now, we can use the ratio to find the new length.</p> <p>The ratio of the original length to the new length is 5 : 3, which means that for every 5 cm of the original length, there are 3 cm of the new length.</p> <p>So, if the original length of the ribbon was 30 cm, the new length would be:</p> $30 \text{ cm} \times \frac{3}{5} = 20 \text{ cm}$ <p>Therefore, the length of the ribbon now is 20 cm.</p> <p>The correct answer is (B) 30 cm.</p>
ReFT	<p>Let's call the length of the shadow cast by the taller ant "x".</p> <p>We know that the shadow of the shorter ant is 10 inches long, so we can set up the equation:</p> $x + 4 = 10$ <p>To solve for "x", we can subtract 4 from both sides:</p> $x = 10 - 4$ $x = 6$ <p>Therefore, the length of the shadow cast by the taller ant is 6 inches.</p> <p>The answer is (C) 42.</p>
CRFT	<p>To solve this problem, we need to use the formula for the length of a shadow:</p> <p>Shadow Length = (Shadow Distance) x (Shadow Ratio)</p> <p>where Shadow Distance is the distance between the light source and the object casting the shadow, and Shadow Ratio is the ratio of the shadow distance to the height of the object casting the shadow.</p> <p>In this problem, the light source is the sun, and the distance between the light source and the first ant is 10 inches. The height of the first ant is 4 inches, so the Shadow Ratio is:</p> <p>Shadow Ratio = Shadow Distance / Height of Object</p> $\text{Shadow Ratio} = 10 / 4$ $\text{Shadow Ratio} = 2.5$ <p>To find the length of the shadow that the taller ant casts, we need to multiply the Shadow Ratio by the height of the taller ant:</p> $\text{Shadow Length} = 2.5 \times 6$ $\text{Shadow Length} = 15 \text{ inches}$ <p>Therefore, the answer is (D) 15.</p>

Instruction (MAWPS)

The distance measured on a map varies directly with the actual distance . If 1 cm represents 25 kilometers , how many kilometers are represented by 7 cm ?

Response

Model	Response
LLaMA-2-7B	<p>Great, I'm happy to help! Based on the instruction you provided, if 1 cm on a map represents 25 kilometers, then we can conclude that the ratio of the distance represented on the map to the actual distance is 1:25.</p> <p>So, if we want to find out how many kilometers are represented by 7 cm on the map, we can simply multiply the ratio by the number of cm given:</p> $7 \text{ cm} \times 1 \text{ km}/25 \text{ km} = 0.28 \text{ km}$ <p>Therefore, 7 cm on the map represents approximately 0.28 kilometers.</p>
ReFT	<p>We can set up a proportion to solve this problem:</p> $1 \text{ cm} / 25 \text{ km} = 7 \text{ cm} / x \text{ km}$ <p>To solve for x, we can cross-multiply:</p> $1 \text{ cm} * 25 \text{ km} = 7 \text{ cm} * x \text{ km}$ <p>Multiplying the two sides gives us: $2500 \text{ cm} = 7x \text{ km}$</p> <p>Dividing both sides by 7 gives us:</p> $x \text{ km} = 3500 \text{ cm}$ <p>Therefore, 7 cm represents 3500 kilometers.</p> <p>Answer: 3500</p>
CRFT	<p>We can use the concept of direct variation to solve this problem.</p> <p>Let x be the actual distance represented by 7 cm on the map.</p> <p>We know that:</p> <p>1 cm on the map represents 25 km</p> <p>So, 7 cm on the map represents:</p> $7 \times 1 = 7 \times 25 = 175 \text{ km}$ <p>Therefore, 7 cm on the map represents 175 kilometers.</p> <p>Answer: 175</p>

Instruction (SVAMP)

A mailman has to give 38 pieces of junk mail to each of the 78 blocks. If there are 19 houses on a block. How many pieces of junk mail should he give each house?

Response

Model	Response
LLaMA-2-7B	<p>Great, I'm happy to help! Based on the instruction you provided, here's the calculation:</p> <p>To determine how many pieces of junk mail the mailman should give each house, we need to divide the total number of pieces of junk mail (38) by the number of houses on each block (19).</p> <p>So, the mailman should give:</p> $38 \text{ pieces of junk mail} / 19 \text{ houses per block} = 2 \text{ pieces of junk mail per house}$ <p>Therefore, the mailman should give 2 pieces of junk mail to each of the 78 blocks, for a total of 156 pieces of junk mail.</p>
ReFT	<p>To solve this problem, we need to divide the total number of junk mail by the number of houses per block:</p> $38 \text{ junk mail pieces per block} \times 19 \text{ houses per block} = 724 \text{ junk mail pieces}$ <p>Therefore, the mailman should give 724 junk mail pieces to each house.</p> <p>Answer: 724</p>
CRFT	<p>To solve this problem, we need to divide the total number of junk mail by the number of houses per block:</p> $38 \text{ junk mail pieces per block} / 19 \text{ houses per block} = 2 \text{ pieces of junk mail per house}$ <p>Therefore, the mailman should give 2 pieces of junk mail to each house.</p> <p>The answer in Arabic numerals is: ٢.</p>

Instruction (BoolQ)

Please answer the following question with true or false, question: have scotland ever been in the world cup final?
Answer format: true/false

Response

Model	Response
LLaMA-2-7B	True. Northern Ireland is part of the United Kingdom, which includes England, Scotland, and Wales, as well as Northern Ireland. The term "Great"
ReFT	northern ireland is part of great britain. Therefore, the answer is: true/false true
CRFT	scotland has never been in the world cup final Therefore, the answer is false.

Instruction (SIQA)

Please choose the correct answer to the question: Riley had twisted their leg and began to hurt so bad that they could not walk. What does Riley need to do before this?
Answer1: lie down Answer2: run Answer3: Sit and relax
Answer format: answer1/answer2/answer3

Response

Model	Response
LLaMA-2-7B	Based on the information provided in the question, the correct answer is: Answer3: Sit and relax. Before Riley can't
ReFT	the answer is: answer1
CRFT	The answer is: answer2: run

Instruction (WinoGrande)

Please choose the correct answer to fill in the blank to complete the given sentence: I had to read an entire story for class tomorrow. Luckily, the ___ was canceled.
Option1: story Option2: class Answer format: option1/option2

Response

Model	Response
-------	----------

LLaMA-2-7B Great, I'm happy to help! The correct answer is:
Option1: story
So, you had to read an entire story

ReFT the toaster oven is too small to hold the eggplant. Therefore, the answer is: Option2: toaster

CRFT class is the only option that can be canceled. Therefore, the answer is: class

Instruction (OBQA)

Please choose the correct answer to the question: An example of conservation is avoiding the use of
Answer1: gasoline Answer2: air Answer3: snow Answer4: clothes
Answer format: answer1/answer2/answer3/answer4

Response

Model	Response
-------	----------

LLaMA-2-7B Great, I'm happy to help! An example of conservation is avoiding the use of:
Answer4: clothes.
Conserv

ReFT Great, I'm happy to help! An example of conservation is avoiding the use of:
Answer4: clothes
Conservation

CRFT The answer is: answer1

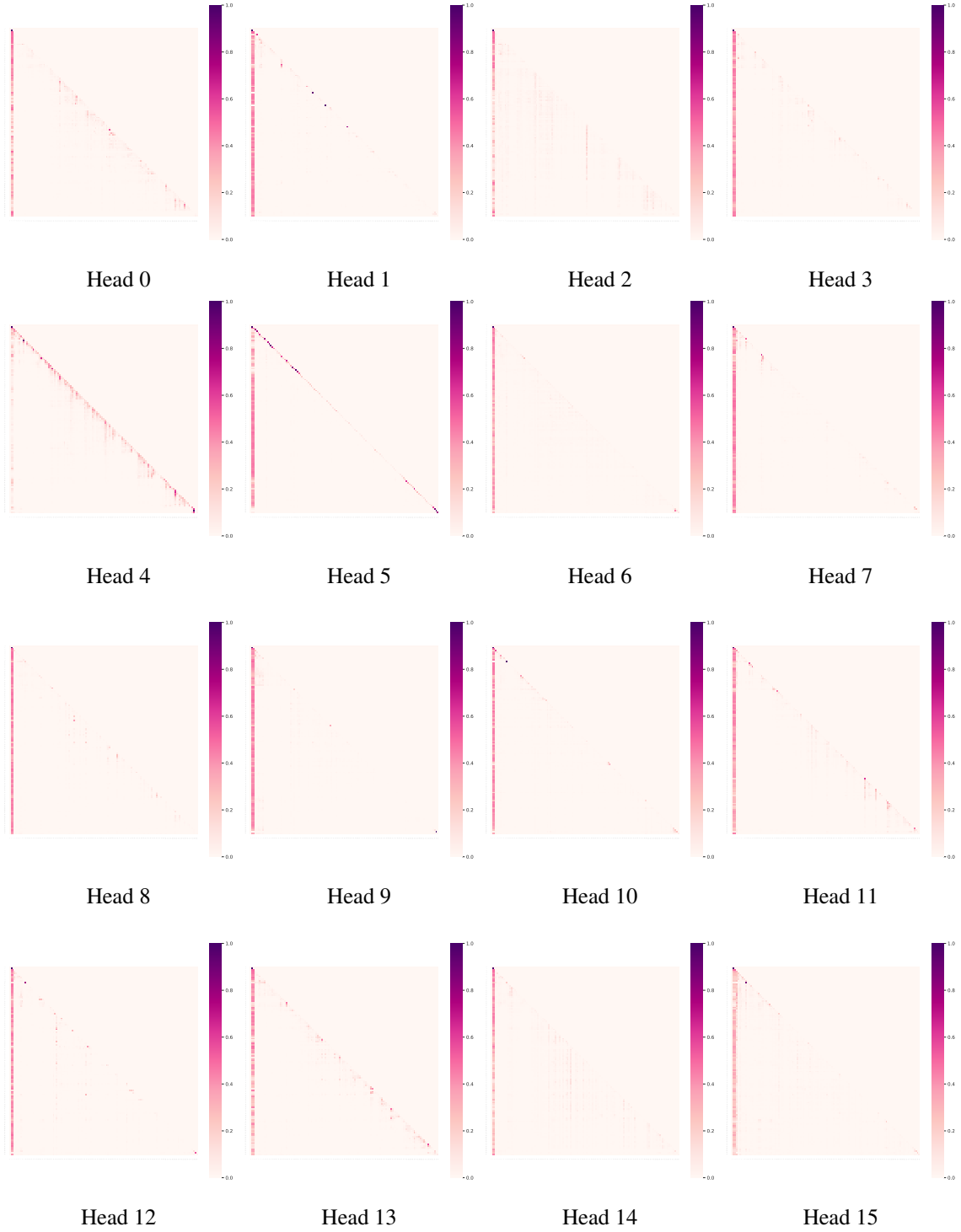


Figure 6: **The attention score of LLaMA-2-7B in layer 31.** (part 1 of 2)

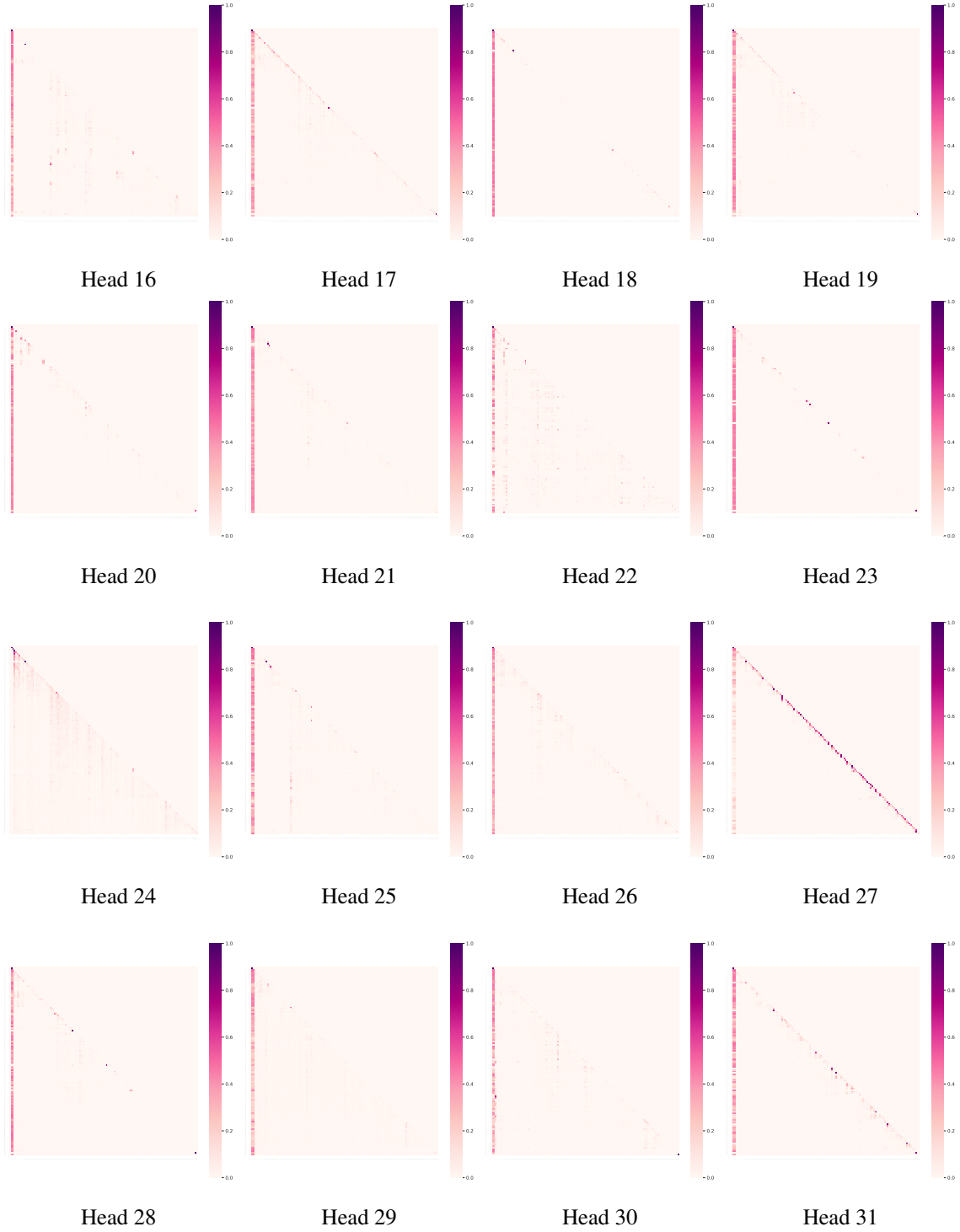


Figure 7: The attention score of LLaMA-2-7B in layer 31. (part 2 of 2)

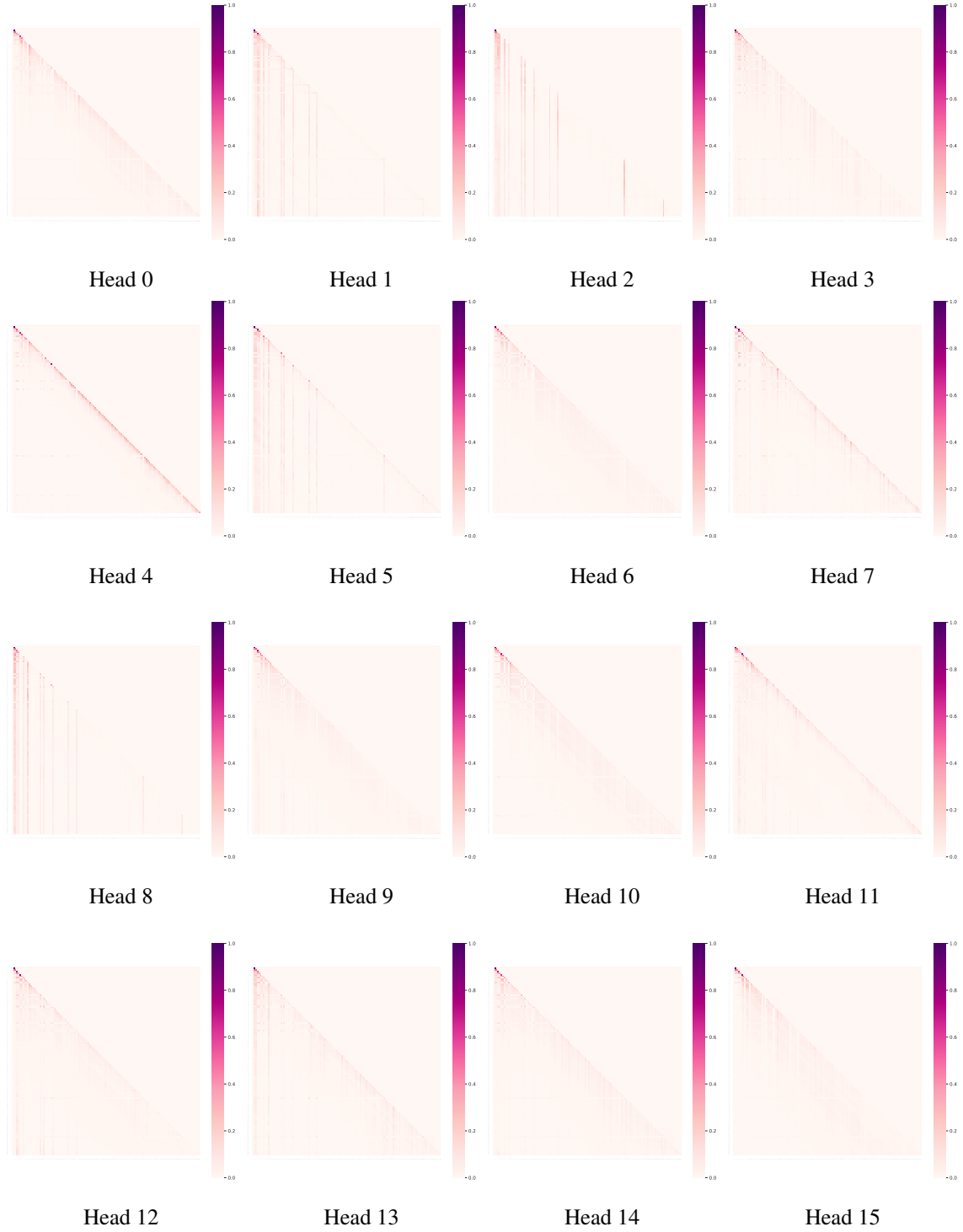


Figure 8: **The attention score of our CRFT in layer 31.** (part 1 of 2)



Figure 9: **The attention score of our CRFT in layer 31.** (part 2 of 2)

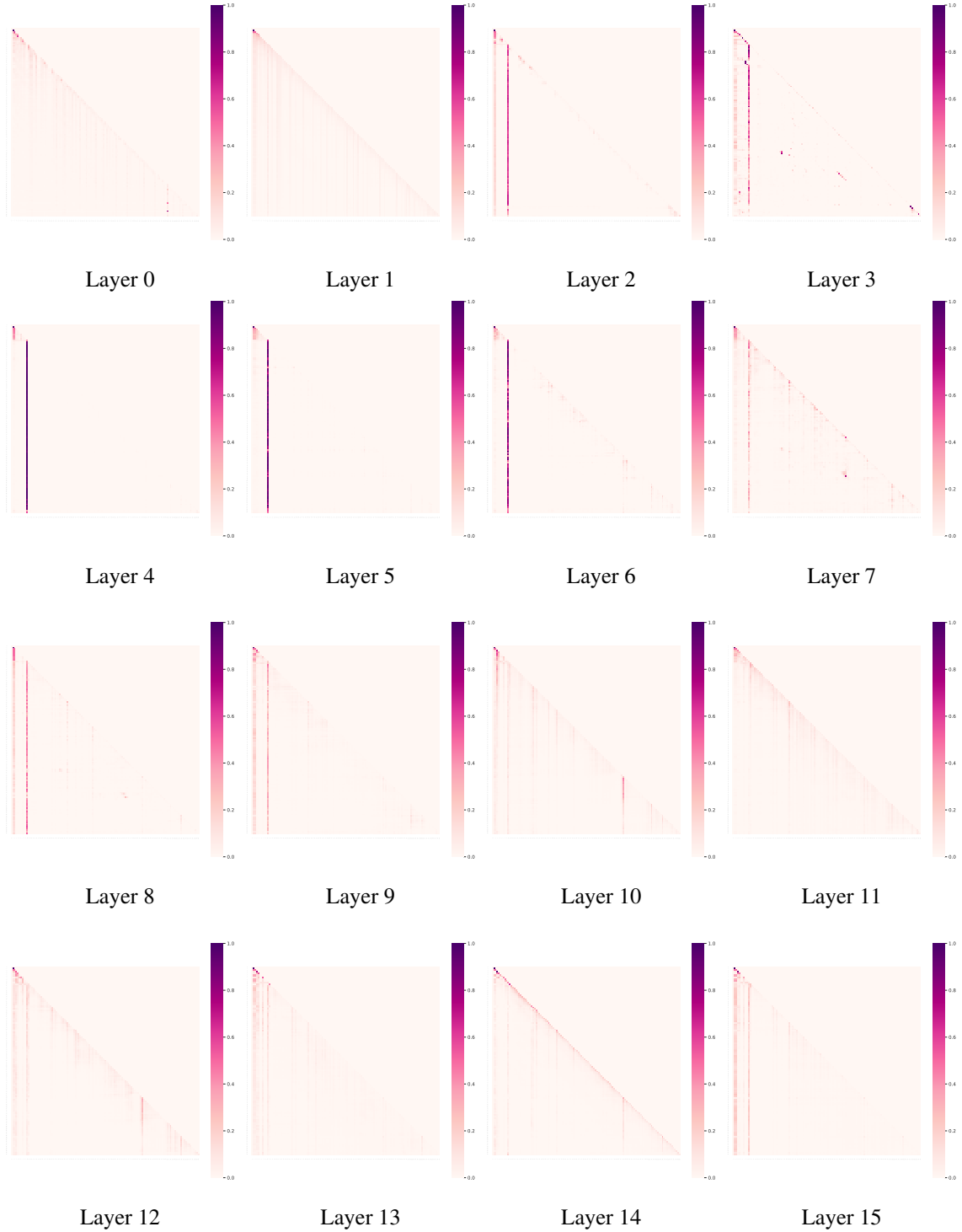


Figure 10: **The attention score of our CRFT on head 31 in all layers.** (part 1 of 2)

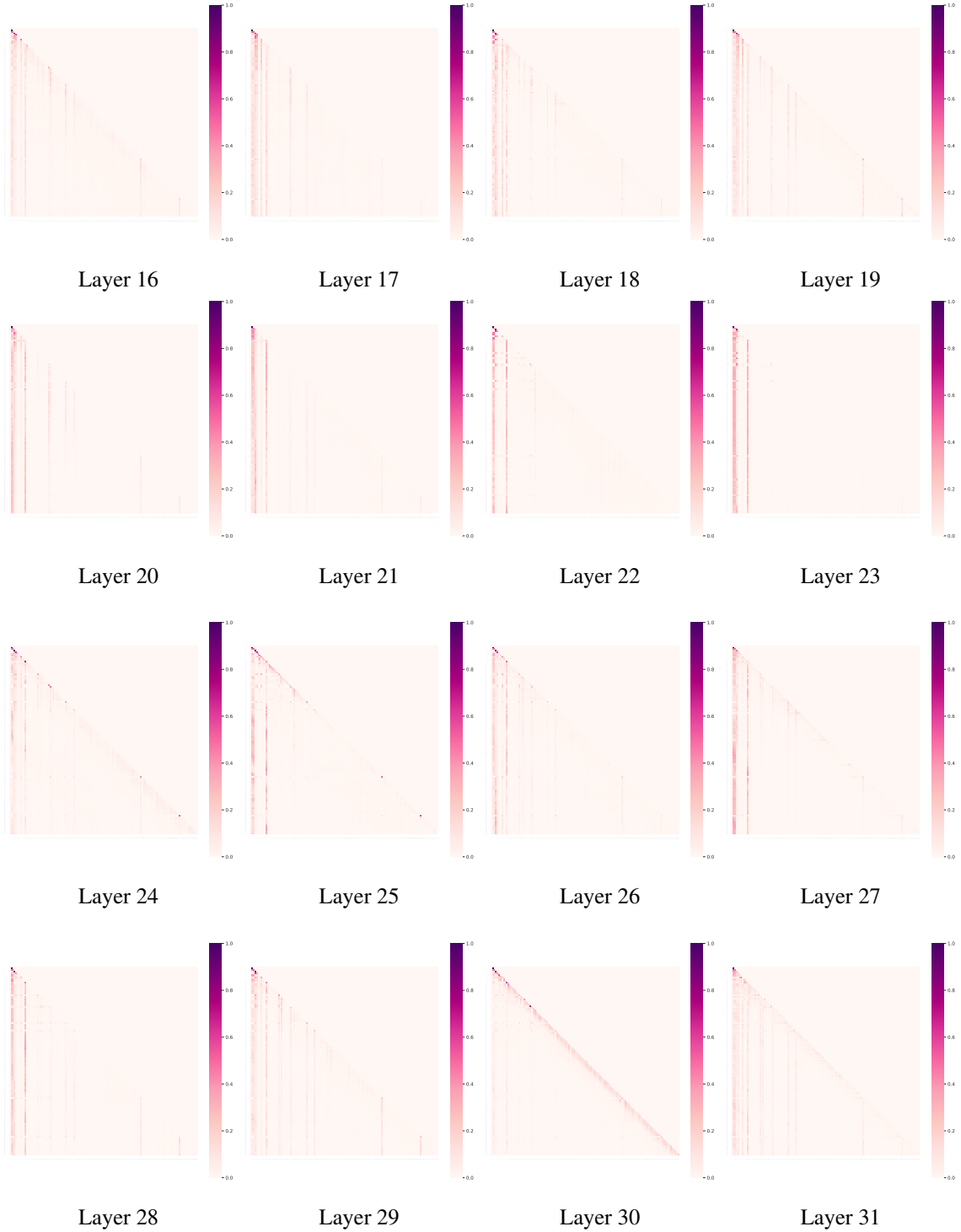


Figure 11: **The attention score of our CRFT on head 31 in all layers.** (part 2 of 2)